Analyst

PAPER

View Article Online
View Journal

Cite this: DOI: 10.1039/d5an01097g

Förster resonance energy transfer-based anion-responsive nanoemulsion optodes: the importance of fluorescent dye liquid lipophilicity and ionophore–dye interaction for stable and background-free anion response

Daiki Matsumoto, Kenji Sueyoshi,† Tatsuro Endo and Hideaki Hisamoto *

In this study, we fabricated and evaluated a highly sensitive Förster Resonance Energy Transfer (FRET)-based anion-responsive nanoemulsion optode (FRET-NE optode) using an originally developed lipophilic fluorescent dye liquid. When the donor (**D**) dye liquid, designed and synthesized for a previously developed poly(vinyl) chloride (PVC) film optode, was directly applied to the NE optode, it was found that the **D** dye liquid leaked into the aqueous phase upon anion response due to insufficient lipophilicity. To address this issue, we designed and synthesized a new **D** dye liquid incorporating a lipophilic alkyl chain. This modification successfully prevented leakage and enabled the construction of a stable FRET-NE optode. However, a new challenge emerged: the fabricated FRET-NE optode exhibited a significant background signal upon mixing with buffer solution. This was attributed to protonation of the acceptor (**A**) dye near the organic–aqueous interface. Upon addition of an anion ionophore, hydrogen-bonding interactions between the **A** dye and the anion ionophore suppressed protonation near the organic–aqueous interface and effectively suppressed the background signal. This paper highlights the critical importance of **D** dye liquid lipophilicity in FRET-NE optode fabrication and demonstrates that hydrogen-bonding interactions between the **A** dye and the anion ionophore are effective in suppressing background signals. The optimized FRET-NE optode composition exhibited approximately 10-fold higher sensitivity compared to conventional non-FRET sensors. These findings suggest that the application of FRET using fluorescent dye liquids holds great promise for dramatically enhancing the sensitivity of conventional NE optodes.

Received 17th October 2025,
Accepted 31st January 2026

DOI: 10.1039/d5an01097g

rsc.li/analyst

Introduction

Various ion detection methods have been developed to date, including electrochemical methods such as ion-selective electrodes (ISEs) and optical methods known as optodes.[1–4] These methods are intended for applications in environmental monitoring, medical diagnostics, and food analysis, where high sensitivity and selectivity are consistently required.[5–8]

In recent years, nanoemulsion (NE) optodes—dispersions of nanoscale oil droplets in water—have garnered increasing attention as an advanced form of film-type ion-selective optodes (ISOs), which have been under development for decades.[9–13] NE optodes are optical chemical sensors in which functional dyes are dissolved in hydrophobic solvents such as bis(2-ethylhexyl) sebacate (DOS) and 2-nitrophenyl *n*-octyl ether (NPOE), both of which have traditionally served as plasticizers in PVC membranes of ISEs and ISOs. The oil droplets containing dyes are dispersed and stabilized in water with surfactants. Compared to film optodes, NE optodes exhibit significantly faster response times due to their much larger specific surface area and diffusion distances.[14–17] Numerous cation and anion sensors based on NE optodes have been reported to date.[18–25]

Our research group has previously developed lipophilic dye liquids that remain liquid at room temperature and utilized their exceptionally high dye concentrations to construct a variety of highly sensitive sensors. These studies include heparin detection based on co-extraction principles,[26] chloride ion sensing,[27] alkaline phosphatase (ALP) detection *via* enzyme reactions at the organic–aqueous interface,[28] and ion exchange-based sensing of Ca^{2+} and Ag^{+} ions.[29,30] More

Department of Applied Chemistry, Graduate School of Engineering, Osaka Metropolitan University, 1-1 Gakuen-cho, Naka-ku, Sakai, Osaka, 599-8531 Japan. E-mail: hisamoto@omu.ac.jp

†Current affiliation: Department of Chemistry, School of Science, Kitasato University, 1-15-1, Kitazato, Minami-ku, Sagamihara-shi, Kanagawa 252-0373, Japan.

recently, we have reported NE-based optodes responsive to perfluorooctanesulfonic acid (PFOS) *via* fluorous interactions,[31] and anomalous response behaviors in K^+-selective, pH-independent NE optodes depending on the ionophore species used.[32]

Among these studies, we discovered that doping a fluorescent **A** dye into a fluorescent **D** dye liquid enables highly efficient Förster Resonance Energy Transfer (FRET) upon excitation of the donor. Using this approach, we achieved an approximately 22-fold sensitivity enhancement in a film-type optode.[33] Efficient FRET generally requires: (i) a sufficiently short donor–acceptor (**D**–**A**) distance (1–10 nm), (ii) optimal orientation factors, and (iii) substantial spectral overlap between the **D** emission and the **A** absorption wavelengths.[34–36] In FRET-type optodes, the **A** dye is "dissolved" directly into the **D** dye liquid. Consequently, the **D**–**A** distance is inherently short, and the **A** dye is surrounded by many **D** dye molecules with various orientations, making the orientation factor highly favourable. Therefore, satisfying condition (iii), spectral overlap, is critical in designing FRET-NE optodes. Additionally, in response mechanisms based on co-extraction, it is considered advantageous for ion extraction if the polarity of the bulk oil droplet is relatively high.

In this study, we investigated the applicability of our previously developed FRET film-type optode to the fabrication of an NE-based optode that satisfies the aforementioned conditions. NE-based optodes are generally regarded as an advanced form of film-type optodes,[17,18] and it has been assumed that functional molecules used in film-type optodes can be readily adapted for NE-based optodes. However, our recent experimental findings have demonstrated that this design concept is not always transferable.[32] In the present work, we began by converting our established FRET film-type optode into an NE-based optode, but significant differences in response stability and background signal intensity were observed. In this paper, we report how these issues were addressed and resolved while maintaining the benefits of highly sensitive detection *via* FRET.

Experimental

Materials and instruments

Reagents. 1-Hydroxypyrene, 1,2-epoxytetradecane, 1,4-butanesultone, 3,5-bis(trifluoromethyl)phenyl isothiocyanate, and tris(2-aminoethyl)amine were purchased from Tokyo Chemical Industry (Tokyo, Japan).

Trihexyl(tetradecyl)phosphonium chloride ([P_{66614}][Cl]) and Pluronic F-127 (F-127) were purchased from Sigma-Aldrich (St. Louis, MO, USA).

Tetrahydrofuran without stabilizer (THF), chloroform, dichloromethane, *n*-hexane, ethyl acetate, methanol, sodium hydride in oil, potassium carbonate, and sodium hydrogen carbonate were purchased from Fujifilm Wako (Kyoto, Japan).

N,*N*-Dimethylformamide (dehydrated) (DMF), chloroform-d_1, 99.8 atom % D ($CDCl_3$), dimethyl sulfoxide-d_6, and 99.9 atom % D (DMSO-d_6) were purchased from Kanto Chemical (Tokyo, Japan).

1,1′,1″-(Nitrilotris(ethane-2,1-diyl))tris(3-(3,5-bis(trifluoromethyl)phenyl)thiourea) (TTU-1) was synthesized by following the reported procedure.[37] Trihexyl(tetradecyl)phosphonium 9-(2-((dodecyloxy)carbonyl)phenyl)-3-oxo-3*H*-xanthen-6-olate ([P_{66614}][12-FL]) and trihexyl(tetradecyl)phosphonium 4-(pyren-1-yloxy)butane-1-sulfonate ([P_{66614}][HP-SO_3]) were synthesized in our previous work.[26,33] Trihexyl(tetradecyl)phosphonium 4-((1-(pyren-1-yloxy)tetradecan-2-yl)oxy)butane-1-sulfonate ([P_{66614}][HPES]) was synthesized in this work. Chemical structures of the materials for NE preparation and the sensing mechanism are shown in Fig. 1.

The details of synthesis and characterization of the compounds are described in the SI [Scheme S1–S3 and Fig. S1–S5].

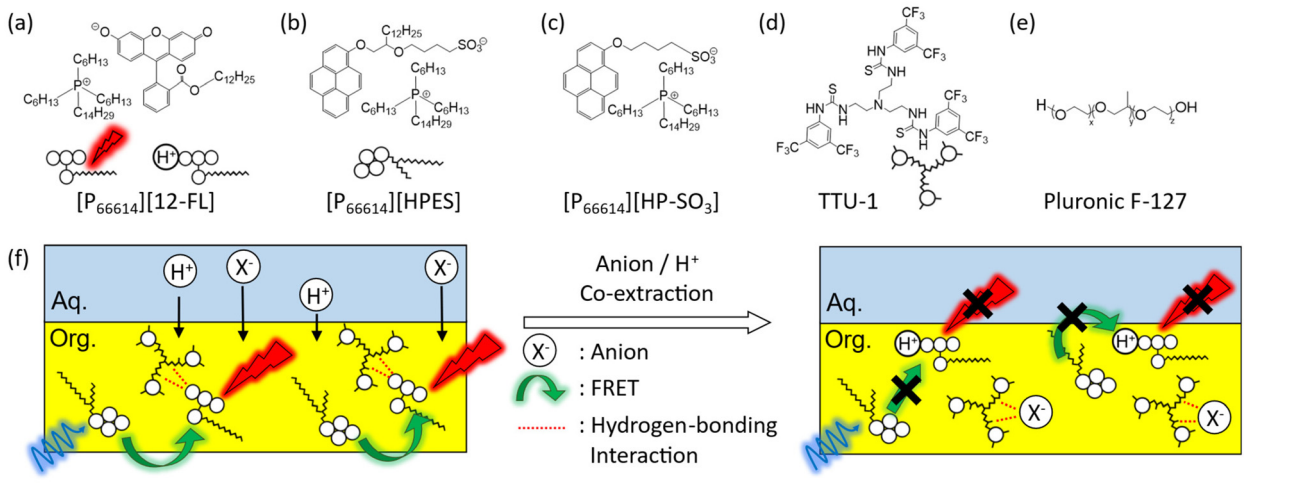

Fig. 1 Chemical structures of the (a) **A** dye ([P_{66614}][12-FL]) (λ_{ex} = 517 nm, λ_{em} = 550 nm), (b) **D** dye liquid ([P_{66614}][HPES] (λ_{ex} = 348 nm, λ_{em} = 498 nm)), (c) **D** dye liquid ([P_{66614}][HP-SO_3]), (d) anion ionophore (TTU-1), and (e) surfactant (Pluronic F-127). (f) Schematic representation of the sensing mechanism near the Aq./Org. phase for the co-extraction of protons and anions.

Instruments. UV-vis absorption spectra were acquired using a JASCO V-730 instrument, whereas fluorescence spectra were collected using a JASCO FP-8550 instrument. Particle sizes were measured by dynamic light scattering (DLS) with a NanoPartica SZ-100V2 (HORIBA, Kyoto, Japan). The interaction between [P_{66614}][12-FL] and TTU-1 was evaluated by proton nuclear magnetic resonance (^{1}H-NMR) measurements (JEOL ECX 400, JEOL, Tokyo, Japan).

Preparation of FRET-NE

FRET-NE without TTU-1. NE was prepared following previously reported methods.[27,28] First, 1.1 mL of a tetrahydrofuran (THF) solution containing the following components was prepared: 2.0 mg mL^{-1} of [P_{66614}][HP-SO_3] or [P_{66614}][HPES] (**D** dye liquid), 0–10 wt% (0–10.7 mol%, *vs.* **D** dye liquid) of [P_{66614}][12-FL] (**A** dye) relative to the **D** dye liquid, and 2.5 mg mL^{-1} of Pluronic F-127 (surfactant). Then, 1.0 mL of this THF solution was injected into 9.0 mL of ultrapure water, followed by sonication for 5 minutes and nitrogen gas purging for 20 minutes to remove the THF. THF removal was confirmed by weight measurements before and after the process. The optimal [**A**]/[**D**] ratio, fluorescence enhancement factor, and FRET efficiency (FE) were determined based on the fluorescence intensity upon mixing with a basic aqueous solution.

Particle size analysis was performed using a NanoPartica SZ-100V2 (HORIBA, Kyoto, Japan) with approximately 2.4 mL of the prepared NE solution. Fluorescence intensity measurements were conducted using a fluorescence spectrophotometer (JASCO FP-8550). The sample solutions were prepared by mixing the FRET-NE solution, ultrapure water, and 100 mM HEPES-NaOH buffer (pH 7.4), 0.2 M NaOH, or 0.2 M HNO_3 in a volume ratio of 135 μL : 1215 μL : 1350 μL (1 : 9 : 10, v/v/v), resulting in final concentrations of 50 mM for the buffer and 0.1 M for NaOH or HNO_3.

FRET-NE with TTU-1. 1.0 mL of THF solution was prepared containing 2.0 mg mL^{-1} of [P_{66614}][HPES], 0.036 mg mL^{-1} (1.8 wt%) of [P_{66614}][12-FL], 2.5 mg mL^{-1} of Pluronic F-127, and 0.35 mg mL^{-1} of TTU-1, corresponding to a tenfold molar excess relative to [P_{66614}][12-FL]. NE was fabricated and evaluated using the same procedure as described above.

Evaluation of the interaction between the anion ionophore (TTU-1) and the anionic acceptor dye ([P_{66614}][12-FL]) based on ^{1}H-NMR analysis and fluorescence intensity

Three sample solutions were prepared by dissolving the following combinations in approximately 0.6 mL of DMSO-d_6: (1) 4.8 mg (4.9 mmol) of [P_{66614}][12-FL] and 6.4 mg (6.6 mmol) of TTU-1, (2) 2.5 mg (2.5 mmol) of [P_{66614}][12-FL] and (3) 2.5 mg (2.6 mmol) of TTU-1. These samples were subjected to ^{1}H-NMR measurements to evaluate the molecular interactions between [P_{66614}][12-FL] and TTU-1. Fluorescence intensity was also assessed by measuring the acid–base response of FRET-NE with and without TTU-1.

Evaluation of anion responses

To evaluate anion responses, a total of 2700 μL of solution was prepared by mixing the FRET-NE solution, ultrapure water, and buffer, NaOH, or HNO_3 in a volume ratio of 135 μL : 1215 μL : 1350 μL (1 : 9 : 10, v/v/v). Aliquots of high-concentration solutions of various anions (sodium salts) were incrementally added to the mixture, and fluorescence measurements were performed to assess the response.

Results and discussion

Preparation of FRET-NE

All NEs prepared in this study yielded particle sizes around 100 nm and polydispersity indices (PDIs) of approximately 0.3 (Fig. S6). As the **D** dye liquid, we initially investigated a pyrene-based ionic liquid, [P_{66614}][HP-SO_3], previously reported in our film-type optode study (Fig. 1(c)).[33] The dye liquid exhibits monomer fluorescence when dissolved in solvents, but in the neat (solvent-free) state, the reduced intermolecular distance leads to the emergence of excimer fluorescence. The excimer emission wavelength overlaps with the absorption wavelength of fluorescein-based dyes, which we initially employed as the **A** dye. This spectral overlap enabled highly efficient FRET in the film-type optode configuration.[33]

The results are shown in Fig. 2(a). Under basic conditions, the **A** dye exists predominantly in its deprotonated form and exhibits fluorescence. In this environment, strong **A** fluorescence based on FRET was observed (λ_{em} = 550 nm). In contrast, under acidic conditions, intense monomer fluorescence

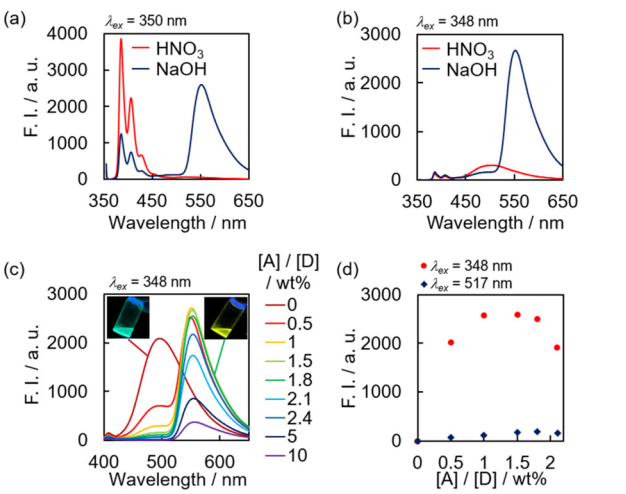

Fig. 2 Fluorescence spectra of the NE composed of (a) [P_{66614}][HP-SO_3], [P_{66614}][12-FL] and the surfactant, (b) [P_{66614}][HPES], [P_{66614}][12-FL] and the surfactant. (c) Fluorescence spectra of NE composed of [P_{66614}][HPES] containing 0–10 wt% [P_{66614}][12-FL] and photographic images taken at 0 mol% and 1.8 mol% [P_{66614}][12-FL] doping under 365 nm UV irradiation. (d) Fluorescence intensity of the NEs composed of different acceptor concentrations (red circles: FRET-NE (λ_{ex} = 348 nm, λ_{em} = 550 nm), dark blue diamond: non-FRET system (direct excitation of **A** dye) (λ_{ex} = 517 nm, λ_{em} = 550 nm).

from pyrene (λ_{em} = 380–400 nm) was detected (Fig. 2(a)). This phenomenon is attributed to the insufficient lipophilicity of [P_{66614}][HP-SO_3], which likely led to ion exchange between nitrate ions and the [HP-SO_3] anion, causing the **D** dye molecules to leak into the aqueous phase. As a result, excimer formation was inhibited and FRET was strongly suppressed.

To address this issue, we newly designed and synthesized [P_{66614}][HPES], a new **D** dye liquid with enhanced lipophilicity through the introduction of long alkyl chains. The fluorescence spectrum of the NE prepared using this molecule is shown in Fig. 2(b). Since the emission spectrum of the **D** dye liquid overlaps with the absorption spectrum of the **A** dye, the system satisfies the abovementioned condition (iii) for efficient FRET in FRET-NE design (Fig. S7).

As observed with [P_{66614}][HP-SO_3], strong **A** fluorescence based on FRET (λ_{em} = 550 nm) and attenuated pyrene excimer fluorescence (λ_{em} = 498 nm) were confirmed under basic conditions (Fig. 2(b)). However, under acidic conditions, only an increase in donor excimer fluorescence (λ_{em} = 498 nm) was observed, with negligible monomer fluorescence. These results indicate that employing a highly lipophilic **D** dye liquid is essential for the successful fabrication of FRET-NE systems. This issue was not encountered in our previously reported plasticized PVC film-based optodes, likely because the hydrophobic nature of PVC and the relatively small organic–aqueous interfacial area allowed [P_{66614}][HP-SO_3] to remain stably retained within the film matrix. The fluorescence enhancement and FRET efficiency (FE) were evaluated based on fluorescence measurements conducted at varying molar ratios of **A** dye to **D** dye liquid ([**A**]/[**D**]), using the following equations:[33,38]

$$\text{fluorescence enhancement} = F_{\mathbf{A}(\lambda\mathbf{D})}/F_{\mathbf{A}(\lambda\mathbf{A})}$$

$F_{\mathbf{A}(\lambda\mathbf{D})}$: **A** fluorescence intensity upon excitation of the **D** dye liquid (λ_{ex} = 348 nm, λ_{em} = 550 nm); $F_{\mathbf{A}(\lambda\mathbf{A})}$: **A** fluorescence intensity upon excitation of the **A** dye (λ_{ex} = 517 nm, λ_{em} = 550 nm).

$$\text{FE} = 1 - F_{\mathbf{D}(\lambda\mathbf{D})}/F_{0(\lambda\mathbf{D})}$$

$F_{\mathbf{D}(\lambda\mathbf{D})}$: **D** excimer fluorescence intensity of FRET-NE with varying **A** compositions (λ_{ex} = 348 nm, λ_{em} = 498 nm); $F_{0(\lambda\mathbf{D})}$: **D** excimer fluorescence intensity of NE prepared using only the **D** dye liquid (λ_{ex} = 348 nm, λ_{em} = 498 nm).

The results are presented in Fig. 2(c), (d) and Fig. S8. At an [**A**]/[**D**] ratio of 1.8 wt%, the fluorescence enhancement reached approximately 14-fold, and the FE was calculated to be around 95%. At 1.5 wt%, the fluorescence enhancement and FE were approximately 15-fold and 92%, respectively; thus, 1.8 wt% was selected as the optimal composition. Assuming that excimer fluorescence arises from a pair of **D** dye molecules, this corresponds to an **A** dye concentration of roughly 4 mol%. This implies that approximately 20–25 excimer pairs surround each **A** dye molecule, suggesting that one acceptor molecule resides within a cubic volume defined by 2–3 excimer pairs per edge length. As shown in Fig. 2(c) (5, 10 wt%) and Fig. 2(d) (above 2 wt%), fluorescence intensity decreased with increasing **A** dye concentration. There are several possible causes for this quenching. Concerning scattering, in this experiment, NE solutions at all **A** dye concentrations were obtained as transparent, precipitate-free solutions, and this remained the case even when diluted during the measurements. Therefore, we believe that there is no decrease in intensity due to light scattering. Regarding the possibility of quenching due to a reduction in excitation light caused by an inner filter effect, considering that the **A** dye concentration is approximately 1/100 of the **D** dye concentration in the liquid, a decrease in intensity due to attenuation of excitation light might be very small. In previous thin-film optode studies,[33] the fluorescence intensity decreased with increasing **A** dye concentration, similar to this study, suggesting that this quenching is dynamic concentration quenching.

Evaluation of the interaction between TTU-1 and [P_{66614}][12-FL] based on fluorescence intensity and ^{1}H-NMR analysis

In the absence of TTU-1, the FRET-NE system exhibited fluorescence intensity under pH 7.4 buffer conditions that was approximately half of that observed under NaOH conditions, resulting in a higher background signal (Fig. 3(a)). The same phenomenon was also observed in our previous absorbance-based nano optode,[27] and it is attributed to protonation of the anionic **A** dye located near the surface of the nano oil droplets. This problem was not observed in the previous thin film experiments.[33] One possible reason for this difference is that in the case of NE optodes, the use of a surfactant can lead to an **A** dye concentration at the oil–water interface, and in the case of thin films, the **A** dye was sufficiently retained by the hydrophobic PVC, resulting in a low dye concentration at the oil–water interface. Our previous work demonstrated that the issue of background signal can be mitigated by introducing hydrogen-bonding anion ionophores into the nano oil droplets.[27] In the present study, instead of using commercial anion ionophores, we employed TTU-1, a compound bearing multiple hydrogen-bonding thiourea groups. Upon preparing

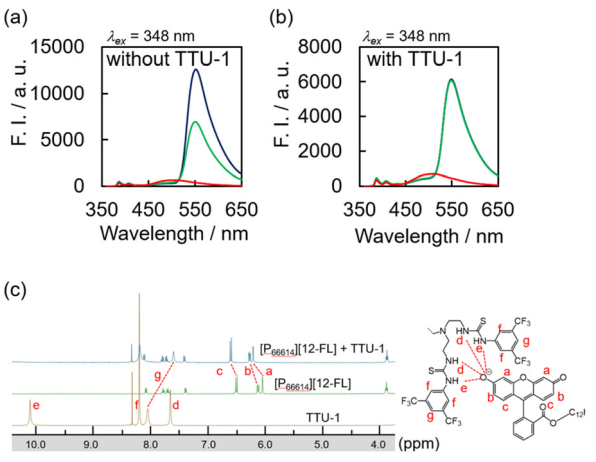

Fig. 3 Fluorescence spectra of FRET-NE (a) without TTU-1, (b) with TTU-1 (blue: base, green: buffer, red: acid). (c) ^{1}H-NMR spectra demonstrating the intermolecular interactions between [P_{66614}][12-FL] and TTU-1 (for simplicity, the structure of TTU-1 is partially omitted).

FRET-NE solutions containing TTU-1 and evaluating their acid–base response, we found that the fluorescence intensity under buffer conditions closely matched that under NaOH conditions (Fig. 3(b)). This suggests that, similar to previous reports, hydrogen-bonding interactions between $[P_{66614}][12\text{-FL}]$ and TTU-1 suppressed protonation of the **A** dye at the organic–aqueous interface. Indeed, the ^{1}H-NMR spectra shown in Fig. 3(c) revealed significant chemical shifts: downfield shifts of protons assigned to positions a, b, and c on the **A** dye, and upfield shifts of protons assigned to position g on the ionophore. These observations support the formation of hydrogen-bonding interactions between the phenolic moiety of the **A** dye and the thiourea groups of the ionophore, consistent with our previous findings.[27] Additionally, the disappearance of peaks assigned to protons d and e is likely due to exchange with deuterium in the solvent or interaction-induced peak broadening resulting from complex formation between the **A** dye and the ionophore. A schematic illustration of the proposed interaction between $[P_{66614}][12\text{-FL}]$ and TTU-1 is also shown in Fig. 3(c).

The observation that the fluorescence intensity of FRET-NE with TTU-1 under NaOH conditions is lower than that of FRET-NE without TTU-1 is attributed to the fluorescence quantum yield of the fluorescein-based **A** dye. Fig. S9 shows the fluorescence spectra of the **A** dye dissolved at equal concentrations in various organic solvents. The dye exhibits relatively strong fluorescence in highly polar solvents, whereas its fluorescence intensity is significantly reduced in low-polarity solvents such as hexane and chloroform. In the presence of TTU-1, a larger proportion of the dye is believed to reside in the bulk phase of the organic droplets, whereas in the absence of TTU-1, the dye is more likely to be localized at the organic–aqueous interface. Since the fluorescence quantum yield of fluorescein is higher in hydrophilic environments such as the organic–aqueous interface than in hydrophobic environments like the interior of organic droplets, the overall fluorescence intensity is greater when TTU-1 is absent.

Evaluation of anion responses

The anion responses of FRET-NE with TTU-1 were evaluated using two excitation wavelengths: one corresponding to the **D** dye and the other to the **A** dye. The results are shown in Fig. 4(a) and (b). The observed anion selectivity followed the Hofmeister series and exhibited clear concentration dependence, indicating that the sensing mechanism is based on co-extraction of protons and anions. Because the NE prepared in this study does not contain PVC, the amount of quaternary phosphonium cations ($[P_{66614}]^+$) is relatively higher than in the case of plasticized PVC thin films. Therefore, we believe that anion extraction by $[P_{66614}]^+$, which is present in large quantities within the oil droplets, is dominant, and the resulting selectivity obtained follows the Hofmeister series. In addition, the large number of sulfonic acid groups present within the oil droplets may make it difficult for the ionophore to exhibit selectivity for specific anions due to competition with the target anions. As a result, the anion selectivity profile was generally consistent with that previously reported for our thin-film optode system.[33] Fig. 4(c) presents the fluorescence spectra obtained during the most responsive ClO_4^- detection using the FRET-based system, while Fig. 4(d) compares the fluorescence intensities with and without FRET. The FRET-based system demonstrated approximately 10-fold higher sensitivity. Regarding improvement of fluorescence intensity, it is possible to obtain a certain level of fluorescence intensity without using FRET by increasing the dye concentration or excitation power. However, as shown in Fig. 2(d), increasing the **A** dye concentration can result in a decrease in intensity due to concentration quenching (NEs prepared using only the **A** dye and surfactant emit almost no fluorescence because of concentration quenching). Furthermore, our method can achieve even stronger fluorescence intensity by increasing the excitation power, making it particularly advantageous for applications in which measuring changes in fluorescence intensity is important, such as monitoring anion concentrations during drug administration. Regarding the concentration range of the calibration curve, no significant changes were observed in Fig. 4(a) and (b). This is somewhat natural, given the difference in whether or not energy transfer from the **D** dye solution is used. However, the shift of the calibration curve toward lower concentrations is an important issue. We believe that improving the anion extraction efficiency is effective in shifting the calibration curve toward lower concentrations, and we plan to investigate the concentration and type of anion ionophore, including selectivity, in the future.

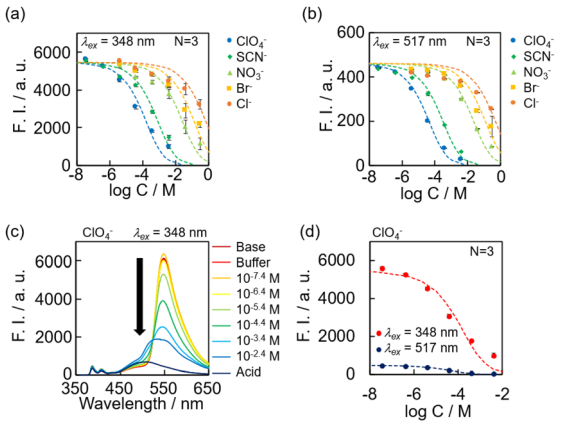

Fig. 4 (a) Response curves of FRET-NE with TTU-1 for various anions (λ_{ex} = 348 nm, λ_{em} = 550 nm) along with theoretical response curves (dashed lines). (b) Response curves of FRET-NE with TTU-1 for various anions (λ_{ex} = 517 nm, λ_{em} = 550 nm) along with theoretical response curves (dashed lines). (c) Fluorescence spectral changes upon addition of ClO_4^-. (d) Fluorescence intensity changes at different excitation wavelengths (λ_{ex} = 348 or 517 nm, λ_{em} = 550 nm) upon addition of ClO_4^-.

Conclusion

This study experimentally demonstrated that lipophilization of the **D** dye liquid is critically important for the fabrication of

FRET-NE optodes. The optimized NE-type optode, with an appropriate [**A**]/[**D**] ratio, exhibited an approximately 15-fold sensitivity enhancement. Background signal interference was effectively suppressed by incorporating a thiourea-based anion ionophore. Furthermore, the final ionophore-incorporated system achieved an approximately 10-fold sensitivity enhancement toward various anions compared to a non-FRET system. These findings suggest that applying this design strategy to conventional NE-based anion sensors could lead to significantly improved sensitivity.

Author contributions

D. M., K. S., T. E. and H. H. conceptualised, planned, and designed the experiments. D. M. and H. H. conceptualised molecular designs. D. M. performed the experiments and analysed the data. D. M., K. S., T. E. and H. H. drafted the manuscript. All authors have approved the manuscript and agree with its submission to this journal.

Conflicts of interest

There are no conflicts to declare.

Data availability

All the experimental data are presented in the main text and supplementary information (SI). Supplementary information is available. See DOI: https://doi.org/10.1039/d5an01097g.

Other information is available upon reasonable request from the corresponding author.

Acknowledgements

This study was partly supported by the KAKENHI 23H01990 (23K26683), the Salt Science Research Foundation and the Iketani Science and Technology Foundation.

References

1 J. Zhai, D. Yuan and X. Xie, *Sens. Diagn.*, 2022, **1**, 213–221, DOI: 10.1039/D1SD00055A.
2 E. Bakker, P. Bühlmann and E. Pretsch, *Chem. Rev.*, 1997, **97**, 3083–3132, DOI: 10.1021/cr940394a.
3 P. Bühlmann, E. Pretsch and E. Bakker, *Chem. Rev.*, 1998, **98**, 1593–1688, DOI: 10.1021/cr970113+.
4 H. Hisamoto and K. Suzuki, *Trends Anal. Chem.*, 1999, **18**, 513–524, DOI: 10.1016/S0165-9936(99)00137-5.
5 S. O. Mirabootalebi and Y. Liu, *Analyst*, 2024, **149**, 3694–3710, DOI: 10.1039/D4AN00334A.
6 A. Barhoum, Y. Alhashemi, Y. M. Ahmed, M. S. Rizk, M. Bechelany and F. M. Adbel-Haleem, *Front. Bioeng. Biotechnol.*, 2024, **12**, 1397587, DOI: 10.3389/fbioe.2024.1397587.
7 C. R. Rousseau and P. Bühlmann, *Trends Anal. Chem.*, 2021, **140**, 116277, DOI: 10.1016/j.trac.2021.116277.
8 B. Li, X. Xie, T. Meng, X. Guo, Q. Li, Y. Yang, H. Jin, C. Jin, X. Meng and H. Pang, *Food Chem.*, 2024, **440**, 138213, DOI: 10.1016/j.foodchem.2023.138213.
9 A. Konefał, P. Piątek, K. Maksymiuk and A. Michalska, *Sens. Actuators, B*, 2023, **391**, 134022, DOI: 10.1016/j.snb.2023.134022.
10 A. A. Mendonsa, T. Z. Sodia and K. J. Cash, *Analyst*, 2024, **149**, 4615–4622, DOI: 10.1039/D4AN00687A.
11 G. Mistlberger, G. A. Crespo and E. Bakker, *Annu. Rev. Anal. Chem.*, 2014, **7**, 483–512, DOI: 10.1146/annurev-anchem-071213-020307.
12 Q. Zhang, X. Wang, V. Decker and M. E. Meyerhoff, *ACS Appl. Mater. Interfaces*, 2020, **12**, 25616–25624, DOI: 10.1021/acsami.0c05379.
13 H. Hisamoto, N. Miyashita, K. Watanabe, E. Nakagawa, N. Yamamoto and K. Suzuki, *Sens. Actuators, B*, 1995, **29**, 378–385, DOI: 10.1016/0925-4005(95)01711-9.
14 S. F. F. S. Yaacob, A. Olasupo and F. B. M. Suah, *Trends Anal. Chem.*, 2024, **171**, 117498, DOI: 10.1016/j.trac.2023.117498.
15 X. Xie and E. Bakker, *Anal. Bioanal. Chem.*, 2015, **407**, 3899–3910, DOI: 10.1007/s00216-014-8413-4.
16 K. Seiler and W. Simon, *Anal. Chim. Acta*, 1992, **266**, 73–87, DOI: 10.1016/0003-2670(92)85281-A.
17 N. Y. Tiuftiakov, K. J. Robinson and E. Bakker, *Electroanalysis*, 2023, **35**, e202200507, DOI: 10.1002/elan.202200507.
18 H. Madawala, S. R. Puri, D. Weaver and J. Kim, *Langmuir*, 2024, **40**, 3004–3014, DOI: 10.1021/acs.langmuir.3c03138.
19 A. L. Dailey, M. D. Greer, T. Z. Sodia, M. P. Jewell, T. A. Kalin and K. J. Cach, *Biosensors*, 2020, **10**, 120, DOI: 10.3390/bios10090120.
20 X. Du and X. Xie, *Sens. Actuators, B*, 2021, **335**, 129368, DOI: 10.1016/j.snb.2020.129368.
21 W. Di and H. A. Clark, *Anal. Methods*, 2020, **12**, 1441–1448, DOI: 10.1039/C9AY02717C.
22 V. Mahendran and J. Philip, *Langmuir*, 2013, **29**, 4252–4258, DOI: 10.1021/la400502b.
23 Q. Chen, X. Li, R. Wang, F. Zeng, J. Zhai and X. Xie, *Anal. Chem.*, 2019, **91**, 10390–10394, DOI: 10.1021/acs.analchem.9b01654.
24 Y. Soda, K. Robinson and E. Bakker, *ACS Sens.*, 2022, **7**, 3108–3115, DOI: 10.1021/acssensors.2c01599.
25 Y. Soda, K. Robinson, R. Nussbaum and E. Bakker, *Chem. Sci.*, 2021, **12**, 15596–15602, DOI: 10.1039/D1SC04930E.
26 T. Mizuta, S. Takai, T. Nishihata, K. Sueyoshi, T. Endo and H. Hisamoto, *Analyst*, 2020, **145**, 5430–5437, DOI: 10.1039/D0AN00335B.
27 K. Maki, R. Oishi, T. Mizuta, K. Sueyoshi, T. Endo and H. Hisamoto, *Analyst*, 2022, **147**, 1529–1533, DOI: 10.1039/D2AN00115B.

28 R. Oishi, K. Maki, T. Mizuta, K. Sueyoshi, T. Endo and H. Hisamoto, *Analyst*, 2021, **146**, 4121–4124, DOI: 10.1039/D1AN00447F.
29 Y. Niwa, T. Mizuta, K. Sueyoshi, T. Endo and H. Hisamoto, *Analyst*, 2019, **144**, 6858–6861, DOI: 10.1039/C9AN01769K.
30 S. Oka, K. Sueyoshi, T. Endo and H. Hisamoto, *Anal. Sci.*, 2023, **39**, 1249–1256, DOI: 10.1007/s44211-023-00337-1.
31 S. Iwamoto, K. Sueyoshi, T. Endo and H. Hisamoto, *Anal. Sci.*, 2024, **40**, 1787–1792, DOI: 10.1007/s44211-024-00603-w.
32 N. Matsumoto, K. Sueyoshi, T. Endo and H. Hisamoto, *Analyst*, 2025, **150**, 3544–3550, DOI: 10.1039/D5AN00516G.
33 T. Mizuta, K. Sueyoshi, T. Endo and H. Hisamoto, *Anal. Chem.*, 2021, **93**, 4143–4148, DOI: 10.1021/acs.analchem.0c05007.
34 H. Q. Peng, L. Y. Niu, Y. Z. Wu, C. H. Tung and Q. Z. Yang, *Chem. Rev.*, 2015, **115**, 7502–7542, DOI: 10.1021/cr5007057.
35 M. Taki, S. Azeyanagi, K. Hayashi and S. Yamaguchi, *J. Mater. Chem. C*, 2017, **5**, 2142–2148, DOI: 10.1039/C6TC05208H.
36 L. Wu, C. Huang, B. P. Emery, A. C. Sedwick, S. D. Bull, X. P. He, H. Tian, J. Yoon, J. L. Sessler and T. D. James, *Chem. Soc. Rev.*, 2020, **49**, 5110–5139, DOI: 10.1039/C9CS00318E.
37 W. Lv, Y. Wang, M. Li, X. Wang and Y. Tao, *J. Am. Chem. Soc.*, 2022, **144**, 23622–23632, DOI: 10.1021/jacs.2c10950.
38 K. Trofymchuk, A. Reisch, P. Didier, F. Fras, P. Gilliot, Y. Mely and A. S. Klymchenko, *Nat. Photonics*, 2017, **11**, 657–663, DOI: 10.1038/s41566-017-0001-7.